Chinese Journal of
POLYMER SCIENCE

RESEARCH ARTICLE

https://doi.org/10.1007/s10118-024-3193-6
Chinese J. Polym. Sci. **2024**, *42*, 1925–1932

Amine-Actuated Catalyst Switch for One-Pot Synthesis of Ether-Ester Type Block Copolymers

Hong Qiu, Peng-Fei Zhang, and Jun-Peng Zhao*

Faculty of Materials Science and Engineering, South China University of Technology, Guangzhou 510640, China

Electronic Supplementary Information

Abstract Organocatalysis has shown special potency for simplifying the construction of complex polymer structures. We are reporting here a one-pot synthetic pathway using amine as a selectivity-switching agent in the two-component catalytic system consisting of triethylborane (Et_3B) and a phosphazene base. We first modelled the interactions of a variety of amines with Et_3B by density functional theory calculations. The results indicate that the aliphatic diamines comprising both primary and tertiary amino groups, capable of forming stable intramolecular hydrogen bonds, undergo the strongest complexation with Et_3B. Accordingly, experimental results demonstrate that the addition of such amines promptly actuates the *in situ* selectivity switch from Lewis pair-catalyzed ring-opening polymerization (ROP) of epoxide (propylene oxide, *n*-butylglycidyl ether, or glycidyl phenyl ether) to organobase-catalyzed ROP of *δ*-valerolactone, allowing one-pot continuous synthesis of ether-ester type block copolymers. We thus exploited the noncovalent interaction between amine and Et_3B to refine the catalyst switch strategy by exempting it from loading of extra catalyst.

Keywords Ring-opening polymerization; Block copolymers; Organocatalysis

Citation: Qiu, H.; Zhang, P. F.; Zhao, J. P. Amine-actuated catalyst switch for one-pot synthesis of ether-ester type block copolymers. *Chinese J. Polym. Sci.* **2024**, *42*, 1925–1932.

INTRODUCTION

With the increasing environmental awareness and the growing demand for metal-free polymeric materials in fields such as biomedicine and electronic device manufacturing, organocatalytic polymerization, especially ring-opening polymerization (ROP), has undergone rapid development over the past two decades, and become the frontier of polymer-related science and technology.[1–3] In addition to the improvement in biocompatibility and environmental friendliness, organocatalysis also exhibits remarkable utilities to enhance reaction rates and selectivity, moderate reaction conditions, broaden substrate applicability, and, in many cases, shorten the synthetic paths to increase overall efficiency and economy for the construction of complex macromolecular architectures.[4] Formulation of such new methods and strategies relies heavily on the discovery and creation of new organocatalytic systems and in-depth understanding of catalytic mechanisms.

Block copolymer represents a class of polymeric materials with high fundamental and practical values due to their inherent ability to self-organize into micro- and nano-sized structures in bulk and solution.[5] Such behavior warrants the widespread utilities of block copolymers as thermoplastic elastomers,[6] surfactants,[7,8] photonic crystals,[9] drug carriers,[10–14] and the crucial components of many high-performance materials.[15] Block copolymers are also featured by extremely diverse and expandable structures and properties, originating from the abundant monomer reservoir and the highly variable fashions of block copolymerization.[4,16,17] However, due to the unique end-to-end connection of the blocky segments, tedious multistep synthesis is often required especially when the polymerization of the constituting monomers are suited to different catalysts.[18–20] The convenient one-pot sequential addition approach is often limited to monomers with similar structures (or the same polymerizing group) that are able to undergo polymerization *via* an identical mechanism.

Reducing the complexity of synthetic steps for block copolymers is a challenging task that polymer chemists need to undertake. A powerful toolkit has been assembled along with the development of organocatalytic polymerization.[21] In particular, the "catalyst switch" strategy has shown special potency transforming epoxide and comonomers into mixed type (multi)block copolymers in one-pot continuous procedures.[19,22–27] For instance, in the Lewis pair type two-component catalytic system constituted by a phosphazene base ($^tBuP_2$) and Lewis acidic triethylborane (Et_3B), the catalytic selectivity for monomers could be promptly switched from epoxide to lactone, or from lactone to epoxide, by *in situ* vari-

* Corresponding author, E-mail: msjpzhao@scut.edu.cn

Received May 5, 2024; Accepted June 10, 2024; Published online August 30, 2024

ation of the acid-to-base ratio, allowing for one-pot synthesis of ether-ester type block copolymers.[25] However, this synthetic strategy has so far been dependent on the addition of extra basic or (Lewis) acidic catalysts to generate the base- or acid-excess catalyst composition required for switching the selectivity to the other monomer.

Complexation of amines and alkylboranes is highly effective[28] and widely used for protecting the latter from air oxidation.[29,30] We previously showed that such a noncovalent interaction could also protect amine from reacting with ethylene oxide, thus fulfilling one-step synthesis of amino-end-functionalized poly(ethylene oxide) directly from amino alcohol initiators.[31] We envisioned that the N-B complexation might also warrant the ineffectiveness of Et_3B in the two-component catalytic system. Therefore, amines could be used to switch the catalyst selectivity from a bifunctional Lewis pair (selective for epoxide) to a predominant base (selective for lactone) so that the addition of extra and expensive ^{t}BuP$_2$ could be omitted.

EXPERIMENTAL

Chemicals

Tetrahydrofuran (THF; Guangzhou Chemical Reagent, 99%) was dried successively by calcium hydride (CaH_2) and *n*-butyllithium before cryo-distilled. 1,4-Benzenedimethanol (BDM; Aladdin, 99%) was dried by azeotropic distillation of THF then dissolved in THF into a 0.5 mol/L solution. *δ*-Valerolactone (VL; Energy chemical, 98%), propylene oxide (PO; Acros Organics, 99.5%), butyl glycidyl ether (BGE; Aladdin, 98%), and glycidyl phenyl ether (GPE; Macklin, 98%) were stirred over CaH_2 at room temperature (RT; *ca.* 25 °C) overnight before distilled. 1-*tert*-Butyl-2,2,4,4,4-pentakis(dimethylamino)-2λ^5,4λ^5-catenadi(phosphazene) (^{t}BuP$_2$; Sigma-Aldrich, 2.0 mol/L in THF), triethylborane (Et_3B; TCI, 1.0 mol/L in THF), and all the amines (Energy chemical, ≥98%) were used as received.

Polymer Synthesis

ROP of VL using amines as actuators

A typical procedure of entry 1 in Table S1 (in the electronic supplementary information, ESI) is as follows. Purified BDM (0.5 mol/L THF solution, 0.22 mmol) and VL (22.0 mmol) were added to a dried Schlenk flask. Pre-mixed Et_3B (1.0 mol/L, 44.0 μL, 0.044 mmol) and ^{t}BuP$_2$ (2.0 mol/L, 11.0 μL, 0.022 mmol) were then added (a small amount of toluene may also be added for improving the solubility of the product), at which point reaction did not occur due to excess of Et_3B over ^{t}BuP$_2$. After the solution was well-stirred, 3-dimethylaminopropylamine (DMAPA; 0.044 mmol) was added. After 3 h, the solidified product was dissolved in THF. A few drops of acetic acid (AcOH) were added for quenching and a small aliquot was withdrawn for ^{1}H-NMR and SEC analysis. Conv.(VL)=98.7%, $M_{n,SEC}$(THF, PS standards) = 21.1 kg·mol^{-1}, $Đ_M$=1.23. ^{1}H-NMR (600 MHz, 25 °C, $CDCl_3$, *δ*, ppm): 7.35 (BDM, —$OCH_2C_6H_4CH_2O$—), 5.11 (BDM, —$OCH_2C_6H_4CH_2O$—), 4.10–4.07 (—$CH_2CH_2CH_2CH_2OCO$—), 2.41–2.31 (—$OCOCH_2CH_2CH_2CH_2$—), 1.74–1.60 (—$OCOCH_2CH_2CH_2CH_2$—).

Synthesis of ether-ester block copolymers from epoxide-lactone mixed monomers

A typical polymerization procedure is given as follows. Purified BDM (0.5 mol/L THF solution, 0.18 mmol), PO (7.1 mmol), and VL (10.7 mmol) were added to a dried Schlenk flask. Then, pre-mixed Et_3B (1.0 mol/L, 54.0 μL, 0.054 mmol) and ^{t}BuP$_2$ (2.0 M, 9.0 μL, 0.018 mmol) were added. At this point, due to the excess of Et_3B over ^{t}BuP$_2$, only PO reacted and VL did not participate. After the mixture was stirred for 12 h, a small aliquot (*ca.* 0.05 mL) was withdrawn and diluted with 0.6 mL of $CDCl_3$ containing one drop of AcOH for ^{1}H-NMR analysis to determine the conversion of PO and VL. The $CDCl_3$ solution was further diluted with THF for SEC analysis to determine $M_{n,SEC}$ and $Đ_M$ of the polymer. Conv.(PO)=100%, Conv.(VL)=0, $M_{n,SEC}$(THF, PS standards)=4.9 kg·mol^{-1}, $Đ_M$=1.06. Then, 0.072 mmol of DMAPA was added. After the reaction mixture was stirred at 25 °C for another 6 h, the solidified product was dissolved in THF. A few drops of AcOH were added for quenching and a small aliquot was withdrawn for ^{1}H-NMR and SEC analysis. Conv.(VL)=94.7%, $M_{n,SEC}$(THF, PS standards)=12.8 kg·mol^{-1}, $Đ_M$=1.10. ^{1}H-NMR (600 MHz, 25 °C, $CDCl_3$, *δ*, ppm): 7.35 (BDM, —$OCH_2C_6H_4CH_2O$—), 5.10 (—PPO—$CH_2CH(CH_3)OCO$—PVL—), 4.56–4.51 (BDM, —$OCH_2C_6H_4CH_2O$—), 4.10–4.07 (—$CH_2CH_2CH_2CH_2OCO$—), 3.69–3.37 (—$OCH_2CH(CH_3)O$—), 2.41-2.31 (—$OCOCH_2CH_2CH_2CH_2$—), 1.74–1.60 (—$OCOCH_2CH_2CH_2CH_2$—), 1.17–1.08 (—$OCH_2CH(CH_3)O$—).

Characterization

Nuclear magnetic resonance (NMR) spectra were recorded at 25 °C on a Bruker AV600 NMR spectrometer using $CDCl_3$ as the solvent and tetramethylsilane as the internal standard. Size exclusion chromatography (SEC) coupled with successively connected UV and refractive index (RI) detectors was conducted in THF at 35 °C using two identical PLgel columns (5 μm, MIXED-C) at a flow rate of 1.0 mL·min^{-1}. For one of the copolymers, SEC coupled with RI and UV detectors was conducted in *N*,*N*-dimethylformamide (DMF) at 35 °C and a flow rate of 1.0 mL·min^{-1} using three successively connected Styragel columns (HR2, HR4, HR6). A series of narrowly distributed polystyrene (PS) standards were used for calibration to obtain apparent number-average molar masses ($M_{n,SEC}$) and molar mass distributions ($Đ_M$) of the (co)polymers.

RESULTS AND DISCUSSION

It has been well-documented that the basicity of ^{t}BuP$_2$ is high enough to trigger the ROP of lactones by activating the hydroxyl groups (or forming alkoxide species) in the initiator or at the propagating chain ends.[25] But when Et_3B is present with equal or excess amount, relatively to ^{t}BuP$_2$, a strong hydroxyl-^{t}BuP$_2$-Et_3B ternary complex is formed which renders poor nucleophilicity of the alkoxide species and transesterification, either on the lactone monomer or the polyester, is strictly inhibited.[32] Therefore, the selectivity-switching agent should have much lower basicity than ^{t}BuP$_2$ so as not to disturb the ^{t}BuP$_2$-catalyzed ROP of lactone, but sufficiently strong interaction with Et_3B to outmatch the ^{t}BuP$_2$-activated alkoxide species so as to capture Et_3B from the hydroxyl-^{t}BuP$_2$-Et_3B ternary complex and restore the activity of the alkoxide species. Therefore, primary amines appear to us as a class of valid candidates.

Considering the complexity of the chemical environments in block copolymerization systems, we first used DFT calculations in a simplified model to measure the structure-related

N-B complexation and screen out, from commercially available primary amines, the optimal selectivity-switching agent(s). Specifically, lower Gibbs free energy (ΔG) indicates more stable amine-Et_3B complex structure.

A variety of primary amines, including simple alkyl ones, ones containing another primary or tertiary amino group, ones containing an alkoxy group, ones containing phenyl groups are involved in the DFT calculation screening (Table 1). According to the calculation results, DMAPA stands out showing the lowest energy upon complexation with Et_3B (ΔG=–45.96 kJ·mol^{-1}) as well as the shortest N-B bond length $l_{(N\text{-}B)}$=166.0 pm (Table 1). We assumed that this is related to its hybrid (primary-tertiary) diamine structure and used DFT calculations to further investigate into the relationship between the structure of this class of diamines and their abilities to complex with Et_3B (Fig. 1).

It is found that when the primary and (*N*,*N*-dimethyl) tertiary amino groups of these hybrid diamines are separated by 2 or 3 carbon atoms, intramolecular hydrogen bonds are

Table 1 DFT calculation results for the complexation of amines and Et_3B.

Amine [a]	$l_{(N\text{-}B)}$ [b] (pm)	ΔG [c] (kJ·mol^{-1})	$l_{(N\text{-}H)}$ [d] (pm)
PA	167.5	–40.85	
HA	167.4	–41.06	
HDA	167.4	–41.30	
DMAPA	166.0	–45.96	199.3
DMEDA	167.1	–42.36	231.7
DEAPA	167.8	–40.12	
THFFA	167.5	–42.19	230.1
2-MOEA	167.8	–39.99	238.8
3-MOPA	168.0	–39.49	
AL	173.1	–31.88	
BzA	167.3	–40.56	
α-MBzA	168.0	–41.04	

[a] Structures and abbreviations of the amines are listed in Fig. 2; [b] Distance between N and B atoms; [c] Gibbs free energy for the interaction between amine and Et_3B; [d] Length of intramolecular hydrogen bond between primary and tertiary amino groups, if any.

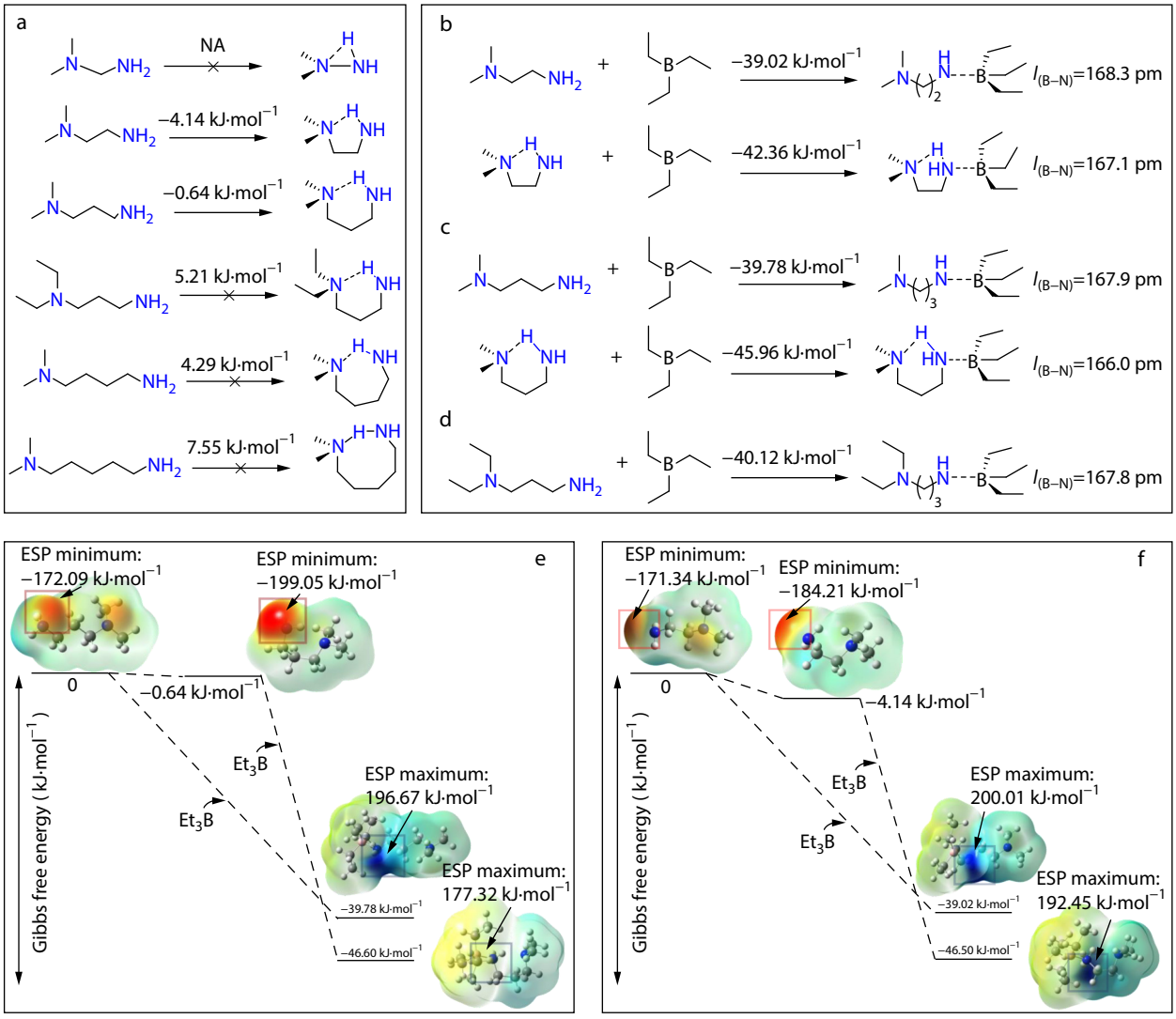

Fig. 1 (a) DFT-calculated Gibbs free energies for the intramolecular hydrogen bonds formed by the hybrid diamines. (b–d) Gibbs free energies and N-B bond lengths for the complexation of Et_3B and the hybrid diamines with or without intramolecular hydrogen bonds. (e, f) Electrostatic potentials and energy profiles for the complexation of Et_3B and the hybrid diamines (e for DMAPA and f for DMEDA).

https://doi.org/10.1007/s10118-024-3193-6

formed spontaneously, arranging the molecules into cyclic structures. The Gibbs free energies are negative when this conformational transition occurs, indicating that the cyclic hydrogen-bonded structures are thermodynamically stable. When the spacing between the primary and tertiary amino groups is only 1 or more than 3 carbon atoms, or when the substituents of the tertiary amino group change into ethyl groups, the ΔG values become positive, indicating that these molecules are unable to spontaneously adopt a cyclic conformation in solution (Fig. 1a). The intramolecular hydrogen bonding is prohibited probably due to the unfavored ring size or overcrowding around the N atom.

The intramolecular hydrogen bonding and formation of cyclic structure may have enhanced the electron-donating ability of the primary amino group, thereby facilitating stronger complexation with the electron-deficient Et_3B. To corroborate such an assumption, we have conducted DFT calculations for the complexation of Et_3B and the hybrid diamines, including DMAPA, *N*,*N*-dimethylethylenediamine (DMEDA), and 3-diethylaminopropylamine (DEAPA) with or without intramolecular hydrogen bonding. It is shown that the Gibbs free energies of complexation with Et_3B decrease for both DMEDA and DMAPA upon cyclization, and that the complexation is stronger in the case of cyclized DMAPA than the cyclized DMEDA (Figs. 1b and 1c). It should be noted that although the ability of DMAPA for intramolecular hydrogen bonding seems somewhat limited (ΔG=−0.64 kJ·mol^{-1}), its complexation with Et_3B may have promoted the formation of the cyclic structure. On the other hand, Et_3B-complexation with the linear form of DEAPA appears slightly stronger as compared with the linear forms of DMAPA and DMEDA, but distinctly weaker than their cyclic forms (Fig. 1d), probably because of the steric effect. The electrostatic potential (ESP) analysis shows that when the conformational change occurs, the critical point of the ESP of DMAPA decreases from −172.09 kJ·mol^{-1} to −199.05 kJ·mol^{-1} (Fig. 1e). In comparison, the ESP of DMEDA decreases less significantly (from −171.34 kJ·mol^{-1} to −184.21 kJ·mol^{-1}; Fig. 1f). Therefore, the six-membered hydrogen-bonded ring structure of DMAPA allows the negative charge in the molecule to distribute more towards the primary amino group. Similarly, ESP distributions of the amine-Et_3B complexes indicate that upon cyclization, DMEDA causes a slight decrease in the ESP maximum of Et_3B from 200.01 kJ·mol^{-1} to 192.45 kJ·mol^{-1} (Fig. 1f), whereas DMAPA allows a considerably more distinct decrease from 196.67 kJ·mol^{-1} to 177.32 kJ·mol^{-1} (Fig. 1e). Clearly, the positive charge of Et_3B can be more effectively dispersed through complexation with DMAPA, which also confirms that DMAPA undergoes stronger complexation as compared with other amines investigated.

Besides, we also calculated for the possibility of intramolecular hydrogen bond formation for primary amines bearing an alkoxy group, including 2-methoxyethylamine (2-MOEA), 3-methoxypropylamine (3-MOPA), and tetrahydrofurfurylamine (THFFA). The results indicate that intramolecular hydrogen bonds can be formed only when the O and N atoms are separated by 2 carbon atoms (Fig. S1 in ESI). In the best case, N-B complexation of cyclized THFFA and Et_3B results in a ΔG of −42.19 kJ·mol^{-1} (Table 1), probably because the cyclic ether structure restricts bond rotation thus increasing the stability of the hydrogen bonding. This value is close to that of DMEDA but still inferior to that of DMAPA (Figs. 1b and 1c). Based on these calculations results, DMAPA appears to be the optimal choice as the selectivity-switching agent.

The DFT calculations are then validated by amine-actuated ROP of VL in the acid-excess Et_3B-BuP_2 Lewis pair catalytic system which is inactive for the ROP of VL. If the amine-Et_3B complexation was strong enough, a rapid switch to base-excess or even base-only catalytic condition would be triggered. Therefore, ROP of VL could be launched upon addition of amine, and the actuating activity of the amine could be reflected by the rate the ROP. Due to the crystallinity of poly(*δ*-valerolactone) (PVL), solidification occurs as a good indication of high VL conversion. The experimental conditions and results are shown in Fig. 2 and Table S1 (in ESI).

The results demonstrate that DMAPA is superior to all the other amines. The reaction mixture becomes distinctly viscous within 30 min after addition of DMAPA, and near complete VL conversion is reached within 3 h (Fig. 2, entry 1 in Table S1 in ESI). In sharp contrast, when DMEDA or DEAPA is added instead, VL conversion reaches only 72.5% in 24 h and 60% in 48 h (entries 3 and 4 in Table S1 in ESI), respectively, indicating that the actuating activities of DMEDA and DEAPA are much lower than that of DMAPA. These experimental results are in good agreement with the DFT calculation results mentioned above, confirming that the stable six-membered cyclic structure formed by DMAPA through intramolecular hydrogen bonding substantially intensifies the N-B complexation for triggering efficient catalyst switch (Fig. 1d).

It is also shown that aniline (AL) is unable to actuate the ROP of VL (Fig. 2, entry 13 in Table S1 in ESI). The phenyl group, connected directly to the amino group, acts as an "electron reservoir" which largely reduces the Lewis basicity of the amino group. This also accords well with the DFT calculation result that the ΔG for the complexation of AL and Et_3B is only −31.88 kJ·mol^{-1} (Table 1). However, the methylene/methine spacer between the phenyl and the amino groups can help alleviate the charge-dispersing effect, as indicated by the occurrence of ROP of VL in the experiments with benzylamine (BzA) and *α*-methylbenzylamine (*α*-MBzA) (Fig. 2, entries 10 and 11 in Table S1 in ESI).

The actuating activities shown by the aliphatic amines containing an alkoxy group are not as good as the hybrid amines. The most active one, THFFA, achieves a VL conversion of only 33.4% in 48 h (Fig. 2, entry 8 in Table S1 in ESI). This may be attributed to the presence of a large number of oxygen-containing species (*e.g.*, esters, THF) that disturbs the intramolecular amino-ether hydrogen bonding. Another possible explanation is that the weak interaction between Lewis basic ether O atom and Et_3B interferes with its complexation with the amino group. Linear aliphatic primary amines also exhibit actuating activities, although not as competitive as DMAPA. For instance, VL conversion reaches nearly 80% in 24 h after addition of *n*-propylamine (PA) (Fig. 2, entry 2 in Table S1 in ESI). Increasing the length of alkyl group causes a decrease in the actuating activity, as VL conversion reaches 40.1% at 48 h in the case of *n*-hexylamine (HA) (entry 5 in Table S1 in ESI). The rate of ROP does not increase significantly

https://doi.org/10.1007/s10118-024-3193-6

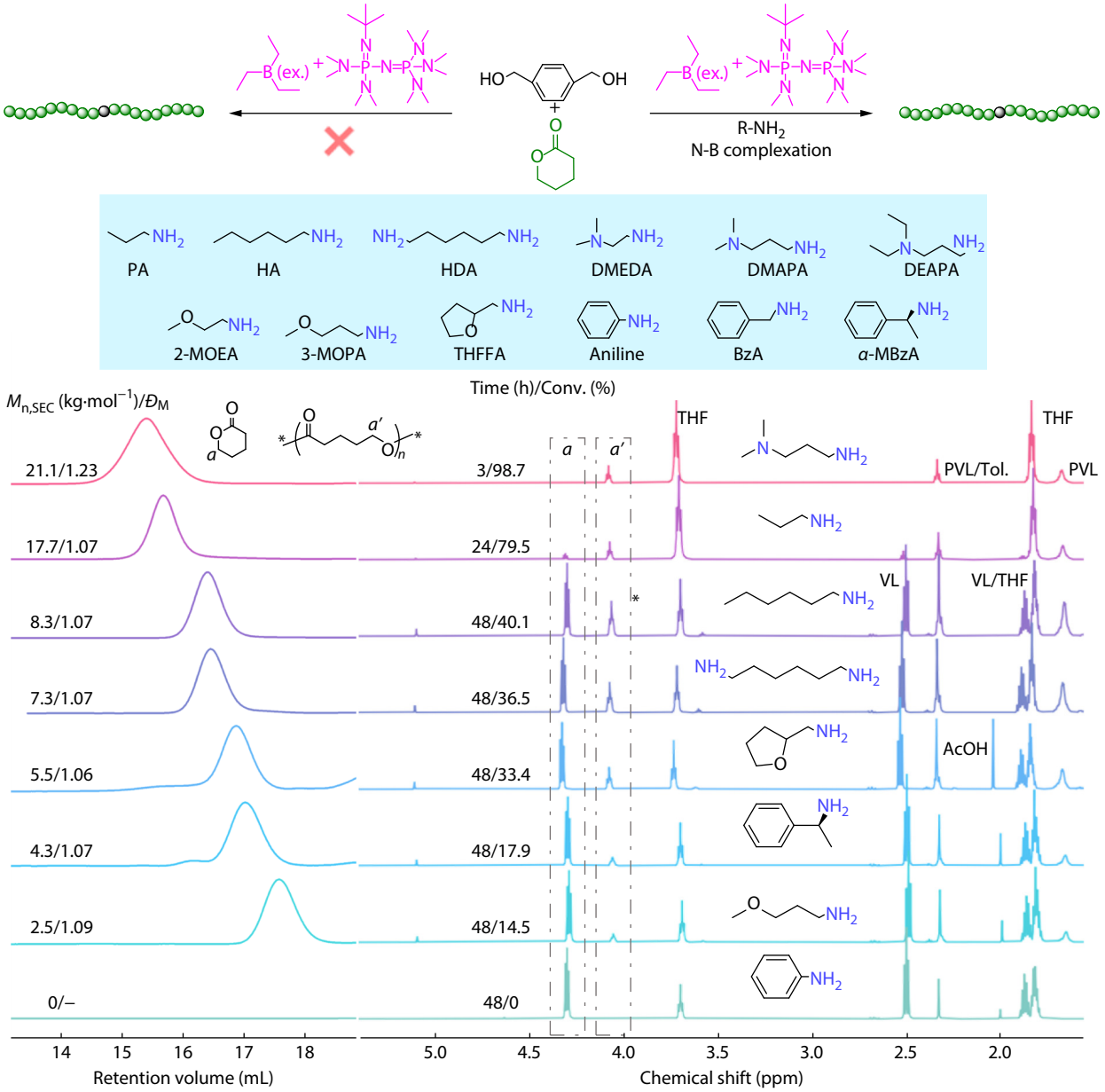

Fig. 2 Schematic illustration (upper), SEC traces (lower left), and ^{1}H-NMR spectra (lower right) for the amine-actuated ROP of VL in the Et_3B-$^tBuP_2$ catalytic system.

when 1,6-hexane diamine (HDA) is employed in 0.5 or 1.0 equiv. of Et_3B (entries 6 and 7 in Table S1 in ESI), indicating that the weakened actuating activity due to longer alkyl groups cannot be compensated by increasing the number of amino functionality or amino concentration. We suppose that the complexation of linear alkyl amines with Et_3B is controlled by kinetics rather than thermodynamics. Namely, longer alkyl groups tend to entangle with the polymer chains, thus limiting the accessibility of the amino group for Et_3B-complexation. Since PA is already the smallest linear alkyl amine that is usable in this system, it is suggested that the strategy of relying solely on kinetic control to intensify the amine-Et_3B complexation is not feasible.

These experimental results have therefore validated the reliability of using DFT calculations to predict and compare the interactions of small molecules such as N-B complexation between amines and Et_3B, especially for compounds that contain analogous substituents. DMAPA is then used as the selectivity-switching agent in the one-pot block copolymerization of epoxide and VL. In a PO-VL mixture containing BDM as the initiator, $^tBuP_2$ and Et_3B are first added in 0.1 and 0.3 equiv. of BDM, respectively, which launches the ROP of PO. Full conversion of PO with controlled molar mass is reached in 12 h (more details can be found in **EXPERIMENTAL** section), while VL has stayed intact (Fig. 3, entry 1 in Table 2). Then, DMAPA is added in a slight excess of Et_3B (*ca.* 0.4 equiv. of BDM). The successful selectivity switch and generation of the expected PVL-*b*-PPO-*b*-PVL triblock copolymer is clearly verified by a VL conversion of 94.7% reached in 6 h, as indicated by ^{1}H NMR spectrum, and increased molar mass with a unimodal distri-

https://doi.org/10.1007/s10118-024-3193-6

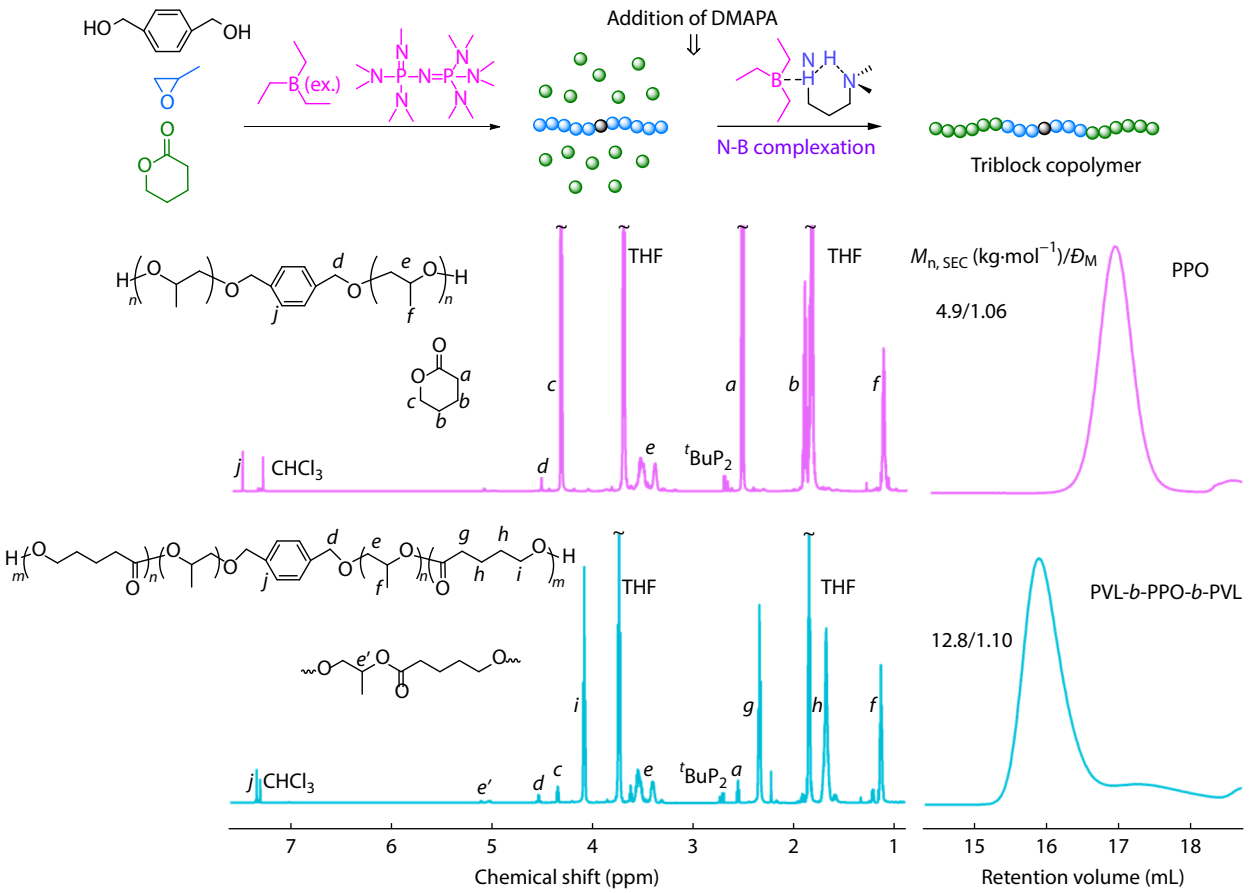

Fig. 3 Schematic illustration (upper) for the one-pot block copolymer synthesis from the mixture of PO and VL in the Et_3B-$^tBuP_2$ catalytic system using DMAPA as a selectivity-switching agent. ^{1}H-NMR spectra (lower left) and SEC traces (lower right) of the products obtained at the two polymerization stages (entry 1 in Table 2).

Table 2 Conditions and results for the one-pot block copolymerization of epoxides and VL through DMAPA-actuated catalyst switch.

Entry	EP	$[EP]_0/[VL]_0/[BDM]_0/[^tBuP_2]/[Et_3B]/[DMAPA]$ [a]	Time (h)	Conv.(EP) [b] (%)	Conv.(VL) [b] (%)	$M_{n,th}$ [c] (kg·mol^{-1})	$M_{n,NMR}$ [d] (kg·mol^{-1})	$M_{n,SEC}$ [e] (kg·mol^{-1})	$Đ_M$ [e]
1	PO	40/60/1/0.1/0.3/0	12	100	0	2.5	2.4	4.9	1.06
		0/0/0/0/0/0.4	6	–	94.7	8.2	8.2	12.8	1.10
2	BGE	40/60/1/0.2/0.6/0	24	100	0	6.0	5.6	5.9	1.08
		0/0/0/0/0/0.8	6	–	96.9	11.8	12.5	13.6	1.38
3	PO	70/90/1/0.2/0.6/0	12	96.6	0	4.1	3.9	6.3	1.06
		0/0/0/0/0/0.8	24	–	9.3	4.9	4.5	6.4	1.07
4	PO+BGE	(90+10)/100/1/0.2/0.6/0	24	97.3	0	6.7	5.9	6.6	1.06
		0/0/0/0/0/0.8	6	–	97.7	16.5	14.0	14.9	1.11
5	GPE	90/100/1/0.3/0.9/0	24	90.5	0	12.3	14.3	9.5	1.08
		0/0/0/0/0/1.2	6	–	99.6	22.3	24.5	26.8	1.34

[a] Molar feed ratio of epoxide (EP), VL, BDM, $^tBuP_2$, Et_3B, and DMAPA; [b] Conversion of epoxide and VL determined by ^{1}H-NMR analysis of the crude products; [c] Theoretical number-average molar mass calculated from monomer-to-initiator ratio; [d] Calculated from ^{1}H-NMR spectrum of the isolated product. [e] Apparent number-average molar mass and molar mass distribution determined by SEC in THF at 35 °C using PS standards. For the second polymerization stage of entry 5, SEC is performed in DMF at 35 °C using PS standards.

bution shown by SEC (Fig. 3).

Therefore, selectivity-switching activity of DMAPA is manifest in the one-pot synthesis of ether-ester block copolymer from mixed monomers of PO and VL. It is worth noting that there are no signals found in the ^{1}H-NMR spectrum that indicate the occurrence of amine-initiated ROP of VL. The shoulder peak observed at the low-molar-mass side may be ascribed to the macromolecular transesterification reaction that is inevitable in strong base-catalyzed ROP of cyclic esters, especially at high monomer conversions.[33] Subsequently, PO is replaced with BGE. DMAPA is added when full conversion of BGE is reached, which actuates the transformation of VL, unreacted during the ROP of BGE, into the PVL segments (Fig. S2 in ESI, entry 2 in Table 2). ^{1}H-NMR spectrum shows that the conversion of VL reaches 96.9% in 6 h, corresponding to the increased molar mass shown by SEC. The broadened molar mass distribution suggests that prompt quenching is necessary to minimize the impact of macromolecular transesterifi-

cation.

When the block copolymerization of PO and VL is conducted with higher monomer-to-initiator ratios, the increased molar mass of PPO segments leads to decreased switching activity of DMAPA. For instance, when the added amount of PO is increased from 40 equiv. to 70 equiv. of BDM, conversion of VL in the second polymerization stage reaches only 9.3% in 24 h even though the catalyst loading is doubled (Table 2 in entry 3). The exact explanation for the length effect of alkyl polyethers is unknown to us yet. Of great interest, when a small amount of BGE (10 equiv. of BDM) is added to react after the ROP of PO, conversion of VL in the third polymerization stage reaches 97.7% in 6 h, also accompanied by distinctly increased molar mass (Fig. S3 in ESI, entry 4 in Table 2). It is then indicated that the installation of intermediate (short) PBGE segments have restored the selectivity-switching activity of DMAPA, despite the even longer PPO segment ($[PO]_0/[BDM]_0 = 90$).

We reason that the challenge of DMAPA capturing Et_3B lies, to a great extent, in the need for breaking the complexation of Et_3B and the oxyanion at the polyether chain end. The strength of O-B complexation may vary according to the pendant group derived from the epoxide monomer. When it is a $ROCH_2-$ type ether group, derived from the glycidyl ether monomer, attached to the *α*-position of the oxyanion and every repeat unit of the polyether chain, the extra ether *O* atoms, with weak Lewis acidity, may tend to complex with Et_3B dynamically, thus disturbing/loosening the complexation of Et_3B with the chain-end oxyanion. Therefore, this relatively less stable O-B complexation makes Et_3B more prone to being captured by DMAPA (Fig. S4 in ESI). Note that the impact of non-terminal pendant (ether) groups may not be excluded. The effect of pendant ether groups facilitating selectivity switch is also showcased when GPE is employed as the epoxide monomer ($[GPE]_0/[BDM]_0$=100; Fig. S5 in ESI, entry 5 in Table 2), which allows VL to be fully polymerized within 6 h in the second stage. Conversion of GPE reaches 90% in the first stage, and the unreacted GPE stays intact during the ROP of VL, confirming stringent selectivity switch of the catalytic system actuated by DMAPA.

CONCLUSIONS

In summary, we exploited the N-B complexation between amines and Et_3B to fulfill one-pot continuous synthesis of ether-ester type block copolymers. Among the 12 amines investigated, DMAPA stands out showing the highest activity to switch the catalytic condition from Et_3B-excess Lewis pair, which inhibits the ROP of VL, to predominant base, thus effectively actuating the ROP of VL. This is attributed, by DFT calculations, to the six-membered cyclic structure formed through intramolecular hydrogen bonding between the primary and tertiary amino groups which substantially intensifies the N-B complexation and facilitates Et_3B capturing from the hydroxyl-^{t}BuP$_2$-Et_3B ternary complex. This feature enables DMAPA to serve as an efficient selectivity-switching agent in the block copolymerization starting from mixed epoxide and VL, in which the ROP rate of VL is also shown to be dependent on the structure of the polyether. This updated catalyst switch strategy is distinctly advantageous over the previous versions in that the selectivity-switching agents, instead of one of the catalytic components, are the structurally simpler and much less costly amines. The DMAPA-borane complexation may be further utilized to smooth other polymer synthesis pathways based on Lewis pair type catalytic systems.

Conflict of Interests

The authors declare no interest conflict.

Electronic Supplementary Information

Electronic supplementary information (ESI) is available free of charge in the online version of this article at http://doi.org/10.1007/s10118-024-3193-6.

Data Availability Statement

The data that support the findings of this study are available from the corresponding author upon reasonable request. The authors' contact information: msjpzhao@scut.edu.cn (J. Z.).

ACKNOWLEDGMENTS

This work was financially supported by the National Natural Science Foundation of China (Nos. 52022031 and 21734004).

REFERENCES

1 Thomas, C.; Bibal, B. Hydrogen-bonding organocatalysts for ring-opening polymerization. *Green Chem.* **2014**, *16*, 1687–1699.
2 Liu, S.; Ren, C.; Zhao, N.; Shen, Y.; Li, Z. Phosphazene bases as organocatalysts for ring-opening polymerization of cyclic esters. *Macromol. Rapid Commun.* **2018**, *39*, 1800485–1800499.
3 Xu, J.; Wang, X.; Liu, J.; Feng, X.; Gnanou, Y.; Hadjichristidis, N. Ionic H-bonding organocatalysts for the ring-opening polymerization of cyclic esters and cyclic carbonates. *Prog. Polym. Sci.* **2022**, *125*, 101484–101508.
4 Hu, S.; Zhao, J.; Zhang, G.; Schlaad, H. Macromolecular architectures through organocatalysis. *Prog. Polym. Sci.* **2017**, *74*, 34–77.
5 Mai, Y.; Eisenberg, A. Self-assembly of block copolymers. *Chem. Soc. Rev.* **2012**, *41*, 5969–5985.
6 Spontak, R. J.; Patel, N. P. Thermoplastic elastomers: fundamentals and applications. *Curr. Opin. Colloid Interface Sci.* **2000**, *5*, 333–340.
7 Alexandridis, P.; Hatton, T. A. Poly(ethylene oxide)-poly (propylene oxide)-poly(ethylene oxide) block copolymer surfactants in aqueous solutions and at interfaces: thermodynamics, structure, dynamics, and modeling. *Colloid. Surface. A* **1995**, *96*, 1–46.
8 Alexandridis, P. Poly(ethylene oxide)/poly(propylene oxide) block copolymer surfactants. *Curr. Opin. Colloid Interface Sci.* **1997**, *2*, 478–489.
9 Stefik, M.; Guldin, S.; Vignolini, S.; Wiesner, U.; Steiner, U. Block copolymer self-assembly for nanophotonics. *Chem. Soc. Rev.* **2015**, *44*, 5076–5091.
10 Gaucher, G.; Dufresne, M.-H.; Sant, V. P.; Kang, N.; Maysinger, D.; Leroux, J. C. Block copolymer micelles: preparation, characterization and application in drug delivery. *J. Control. Rel.* **2005**, *109*, 169–188.

11 Allen, C.; Maysinger, D.; Eisenberg, A. Nano-engineering block copolymer aggregates for drug delivery. *Colloid. Surface. B* **1999**, *16*, 3–27.
12 Kataoka, K.; Harada, A.; Nagasaki, Y. Block copolymer micelles for drug delivery: design, characterization and biological significance. *Adv. Drug. Deliver. Rev.* **2012**, *64*, 37–48
13 Adams, M. L.; Lavasanifar, A.; Kwon, G. S. Amphiphilic block copolymers for drug delivery. *J. Pharm. Sci.* **2003**, *92*, 1343–1355.
14 Rösler, A.; Vandermeulen, G. W. M.; Klok, H. A. Advanced drug delivery devices *via* self-assembly of amphiphilic block copolymers. *Adv. Drug. Deliver. Rev.* **2012**, *64*, 270–279.
15 Hadjichristidis, N.; Pispas, S.; Floudas, G., in *Block copolymers: synthetic strategies, physical properties, and applications*, John Wiley & Sons, Hoboken, NJ, **2003**.
16 Hadjichristidis, N.; Iatrou, H.; Pitsikalis, M.; Mays, J. Macromolecular architectures by living and controlled/living polymerizations. *Prog. Polym. Sci.* **2006**, *31*, 1068–1132.
17 Hadjichristidis, N.; Pitsikalis, M.; Pispas, S.; Iatrou, H. Polymers with complex architecture by living anionic polymerization. *Chem. Rev.* **2001**, *101*, 3747–3792.
18 Ladelta, V.; Zapsas, G.; Abou-Hamad, E.; Gnanou, Y.; Hadjichristidis, N. Tetracrystalline tetrablock quarterpolymers: four different crystallites under the same roof. *Angew. Chem. Int. Ed.* **2019**, *58*, 16267–16274.
19 Zhang, P.; Ladelta, V.; Abou-hamad, E.; Müller, A. J.; Hadjichristidis, N. Catalyst switch strategy enabled a single polymer with five different crystalline phases. *Nat. Commun.* **2023**, *14*, 7559–7569.
20 Ekizoglou, N.; Hadjichristidis, N. Synthesis of model linear tetrablock quaterpolymers and pentablock quintopolymers of ethylene oxide. *J. Polym. Sci., Part A: Polym. Chem.* **2002**, *40*, 2166–2170.
21 Zhao, J.; Pahovnik, D.; Gnanou, Y.; Hadjichristidis, N. A "catalyst switch" strategy for the sequential metal-free polymerization of epoxides and cyclic esters/carbonate. *Macromolecules* **2014**, *47*, 3814–3822.
22 Scheuermann, S.; Kretz, T.; Vitze, H.; Bats, J. W.; Bolte, M.; Lerner, H.-W.; Wagner, M. Redox-active *p*-quinone-based bis(pyrazol-1-yl)methane ligands: synthesis and coordination behaviour. *Chem. Eur. J.* **2008**, *14*, 2590–2601.
23 Xia, Y.; Chen, Y.; Song, Q.; Hu, S.; Zhao, J.; Zhang, G. Base-to-base organocatalytic approach for one-pot construction of poly(ethylene oxide)-based macromolecular structures. *Macromolecules* **2016**, *49*, 6817–6825.
24 Chen, Y.; Song, Q.; Zhao, J.; Gong, X.; Schlaad, H.; Zhang, G. Betulin-constituted multiblock amphiphiles for broad-spectrum protein resistance. *ACS Appl. Mater. Interfaces* **2018**, *10*, 6593–6600.
25 Liu, S.; Bai, T.; Ni, K.; Chen, Y.; Zhao, J.; Ling, J.; Ye, X.; Zhang, G. Biased Lewis pairs:a general catalytic approach to ether-ester block copolymers with unlimited ordering of sequences. *Angew. Chem. Int. Ed.* **2019**, *58*, 15478–15487.
26 Zhao, J.; Pahovnik, D.; Gnanou, Y.; Hadjichristidis, N. One-pot synthesis of linear- and three-arm star-tetrablock quarterpolymers via sequential metal-free ring-opening polymerization using a "catalyst switch" strategy. *J. Polym. Sci., Part A: Polym. Chem.* **2015**, *53*, 304–312.
27 Zhao, J.; Hadjichristidis, N. Polymerization of 5-alkyl δ-lactones catalyzed by diphenyl phosphate and their sequential organocatalytic polymerization with monosubstituted epoxides. *Polym. Chem.* **2015**, *6*, 2659–2668.
28 Sonnenschein, M. F.; Webb, S. P.; Redwine, O. D.; Wendt, B. L.; Rondan, N. G. Physical and chemical probes of the bond strength between trialkylboranes and amines and their utility as stabilized free radical polymerization catalysts. *Macromolecules* **2006**, *39*, 2507–2513.
29 Pihko, P. M., in *Hydrogen bonding in organic synthesis*, John Wiley & Sons, Weinheim, **2009**.
30 Raynal, M.; Ballester, P.; Vidal-Ferran, A.; van Leeuwen, P. W. N. M. Supramolecular catalysis. Part 1: Non-covalent interactions as a tool for building and modifying homogeneous catalysts. *Chem. Soc. Rev.* **2014**, *43*, 1660–1733.
31 Chen, Y.; Zhang, P.; Liu, S.; Pahovnik, D.; Žagar, E.; Zhao, J.; Zhang, G. Noncovalent protection for direct synthesis of α-amino-ω-hydroxyl poly(ethylene oxide). *ACS Macro Lett.* **2021**, *10*, 737–743.
32 Chen, Y.; Shen, J.; Liu, S.; Zhao, J.; Wang, Y.; Zhang, G. High efficiency organic Lewis pair catalyst for ring-opening polymerization of epoxides with chemoselectivity. *Macromolecules* **2018**, *51*, 8286–8297.
33 Zhao, N.; Ren, C.; Shen, Y.; Liu, S.; Li, Z. Facile synthesis of aliphatic ω-pentadecalactone containing diblock copolyesters via sequential ROP with L-lactide, ε-caprolactone, and δ-valerolactone catalyzed by cyclic trimeric phosphazene base with inherent tribasic characteristics. *Macromolecules* **2019**, *52*, 1083–1091.

https://doi.org/10.1007/s10118-024-3193-6